Bachelor End Project

A Study of Chiral Induced Spin Selectivity by means of a Computer Simulation

by

Annick Teepe

Submitted in partial fulfillment of the requirements for the degree of
Bachelor of Science Applied Physics,
at the Delft University of Technology,
to be defended publicly on Wednesday February 13, at 15:00 h.

Student number: 4481569
Project duration: September 1, 2018 – February 13, 2019
Thesis committee: Dr. J. M. Thijssen, TU Delft, supervisor
Dr. M. T. Wimmer, TU Delft

TU Delft

Abstract

In this research, the effect of Chiral Induced Spin Selectivity is studied by means of a transport calculation on a model of a chiral molecule between two gold contacts. The method consists of two main parts: optimizing the geometry of the entire system, being the molecule and the contacts, and performing the transport calculation on the system, which yields the density of states and the transmission over the energy range of -0.5 to 0.0 Hartree.

The geometry optimization is performed in two ways: in the first approach the entire system is optimized under the constraints that the y- and z-coordinates of the atoms of the contacts are frozen, in the second approach the atoms of the contacts are completely frozen on their initial positions. The first approach did not conserve the periodic structure of the gold lattice. The second approach yielded a geometrically optimized system with correct contacts.

The transport calculation is performed on the three systems, being the non-optimized system, the system optimized by the first method and the system optimized by the second method. There was no spin selectivity found: the density of states as well as the transmission are exact copies for the two spin orientations, which is the consequence of a spin-restricted transport calculation.
The density of states for the three systems are similar. The highest occupied molecular orbital as well as the lowest unoccupied molecular orbital were found to be situated just below and above the Fermi energy of the contacts, respectively, which is consistent with literature.
The transmission of the three systems show greater variation. The systems with optimized geometries have a constant transmission close to zero around the Fermi energy of the contacts. The non-optimized system has a fluctuating transmission above zero around this energy.

Based on these findings, a spin-unrestricted transport calculation including a spin-orbit ZORA-key is proposed. In order to speed up calculations, it is also recommended to apply the Wide Band Limit.

Contents

1 Introduction

In this research, the effect of Chiral Induced Spin Selectivity (CISS) will be studied by performing a transport calculation on a model of a chiral molecule sandwiched between two gold contacts. The method consists of two main parts: optimizing the geometry of the system, being the molecule and the contacts, and performing the transport calculation on the system.

Experimental evidence has shown that an electric current passing through ordered films of chiral organic molecules on a surface can lead to remarkably high spin polarization, an effect which has been named CISS [1][2][3]. The spin polarization (P) is defined as

$$P = \frac{j_\uparrow - j_\downarrow}{j_\uparrow + j_\downarrow},$$

where $j_{\uparrow,\downarrow}$ are the currents associated with each spin. This was an unexpected finding since spin-selective electron transport was previously only found in magnetic materials or materials that have large spin-orbit coupling; two properties that organic chiral molecules do not posses.

The fundamental property of spin has both important theoretical implications and practical applications, which make it essential in our understanding of phenomena like magnetism or many-body physics. Applications of spin include devices like MRI scanners, spin transistors or spin quantum computers. The effect of CISS opens exciting possibilities, such as the use of chiral molecules in spintronics applications, and it provides a better understanding of spin-selective processes in biology - it may even help to explain how weak magnetic fields affect navigation by birds and fish [1].

In the chapter Theory, a short overview of the theory of quantum mechanics will be given, as well as the basics of the mathematical description and analysis of a many-body problem. The effect of CISS shall be explained additionally. Next, the chapter Models and Results contains the simulation that explores the effect of CISS and the results obtained from them. Finally, the main conclusions and some discussion points will be presented in the chapter Conclusions and Discussion.

This research has been performed as part of the Bachelor Applied Physics program of the Delft University of Technology.

2 Theory

In this chapter the theory underlying the CISS effect in a computer simulation is given: this theory forms the background of the model of, and the calculations on, a helicene molecule between two contacts. First an overview of the theory of quantum mechanics is given, with emphasis on the meaning of spin and the mechanism of the spin-orbit interaction. The mathematical description and the analysis of a many-body problem is included in the second section. The third section includes the explanation of the CISS effect itself.

2.1 Overview Quantum Mechanics

Quantum mechanics is a physical theory that describes the behavior of matter and energy with interactions of quanta (e.g. an electron or a photon) on an atomic and subatomic scale. To describe the evolution of the state of a mechanical system, vectors are introduced. These vectors describe the state of the particles in the system, and live in the so-called Hilbert space, a complex vector space in which an inner product is defined. They are represented by a ket-vector: $|\psi\rangle$.

2.1.1 Schrödinger equation

The time evolution of the state of a system is governed by the time-dependent Schrödinger equation (TDSE). For a spinless particle of mass m in a potential $V(\mathbf{r})$ this equation reads:

$$i\hbar\frac{\partial}{\partial t}|\Psi(\mathbf{r},t)\rangle = -\frac{\hbar^2}{2m}\nabla^2|\Psi(\mathbf{r},t)\rangle + V(\mathbf{r})|\Psi(\mathbf{r},t)\rangle\,. \tag{1}$$

Here, $\hbar$ is the Planck's constant, $\frac{\partial}{\partial t}$ the partial derivative with respect to the time t and ∇^2 the Laplace operator. This equation can be shortened by introducing the Hamiltonian operator, $\hat{H}$. This operator is Hermitian [1]. The equation then takes the following form:

$$i\hbar\frac{\partial}{\partial t}|\Psi(\mathbf{r},t)\rangle = \hat{H}|\Psi(\mathbf{r},t)\rangle\,. \tag{2}$$

The solution of the TDSE is simple when the state of the system at $t = 0$ is known. This state can be written as a linear combination of the eigenstates of the Hamiltonian, e.g. $|\Psi(\mathbf{r},0)\rangle = \sum_j c_j|\psi_j\rangle$ with the $|\psi_j\rangle$ satisfying the condition $\hat{H}|\psi_j\rangle = \epsilon_j|\psi_j\rangle$ where the c_j are constants and the ϵ_j are the energies.The solution of the TDSE is then given by the following equation:

$$|\Psi(\mathbf{r},t)\rangle = \sum_j c_j e^{-i\epsilon_j t/\hbar}|\psi_j\rangle\,. \tag{3}$$

The Schrödinger equation forms the backbone of quantum mechanics, and can be used to describe numerous different properties of particles, including spin. [4]

2.1.2 Spin

When speaking of spin in classical mechanics, the angular momentum associated with motion about the center of mass is meant; for example the daily rotation of the earth about the north-south axis. The standard form of angular momentum is the orbital angular momentum, defined as $\mathbf{L} = \mathbf{r}\times\mathbf{p}$. Here, $\mathbf{r}$ is the position vector of the particle, and $\mathbf{p}$ is the momentum vector. In quantum mechanics, elementary particles have in addition an intrinsic form of the angular momentum, defined as the spin $\mathbf{S}$.

Every elementary particle has a specific value of the spin; photons have spin 1, electrons have spin 1/2, and so on. In this research, we deal with spin-1/2 electrons. Particles with a half-integer spin quantum number are called fermions, hence electrons belong to this class. Fermions can have two different spin

[1] The operator $\hat{A}$ is Hermitian when it satisfies the equation: $\langle f|\hat{A}|g\rangle = (\langle g|\hat{A}^\dagger|f\rangle)^*$ for all $f(x)$ and $g(x)$, with * the complex conjugate, and $\dagger$ the Hermitian conjugate

orientations, which are represented by a spin-up ket $\left|\frac{1}{2}\frac{1}{2}\right\rangle$ and a spin-down ket $\left|\frac{1}{2}-\frac{1}{2}\right\rangle$. The numbers inside these kets are the quantum number for spin, s, and the so-called magnetic quantum number, m_s, respectively.

When a measurement of the spin of an unpolarized single particle takes place, there is an equal probability of finding it in the spin-up state or spin-down state. This can be understood by noticing that before measurement, the orientation of the spin is both up and down; the measurement forces the particle to choose a state. [5]

2.1.3 Spin-Orbit Interaction

An electron orbiting the nucleus is a moving charged particle. From the field of electrodynamics we know that a moving charge induces a magnetic field. Now, an electron orbiting a proton will be considered. Two reference frames can be used: from the electron point of view, the proton is circling around it, while from the proton point of view, the electron is the one that moves. In each case, the moving charge sets up a magnetic field **B**. The reference frame of the electron will be used.

The electron has a magnetic dipole moment, μ, which is proportional to its spin, according to $\boldsymbol{\mu} = \gamma \mathbf{S}$. Here, γ is the so-called gyro-magnetic ratio, which is the ratio of the magnetic moment to the angular momentum. Due to the magnetic field created by the moving proton, a torque $\tau = \boldsymbol{\mu} \times \mathbf{B}$ is exerted on this magnetic moment. This torque tends to align parallel to the field.

The (potential) energy associated with the torque is given by $\hat{H} = -\boldsymbol{\mu} \cdot \mathbf{B}$. Here, **B** is proportional to the orbital angular momentum **L**, and as explained above the magnetic moment is proportional to the spin. This means that the energy is proportional to the inner product of the spin and the angular momentum, thus we arrive at the spin-orbit interaction within an atom. The official derivation is described in [4], in the chapter covering the Dirac Equation. The result is the following equation:

$$\hat{H}_{SO} \propto \frac{1}{r}\frac{\delta V}{\delta r}\mathbf{S}\cdot\mathbf{L}. \tag{4}$$

Simply stated, the spin-orbit interaction is due to the magnetic field generated by the proton that exerts a torque on the magnetic dipole moment of the electron. [5][6]

2.2 Many-body problem

When dealing with a large number of particles in physics, the problem usually becomes too complicated to be solved exactly. The complexity of the problem is directly clear from the Hamiltonian for N electrons and K nuclei, which reads, in atomic units:

$$H = \sum_{i=1}^{N} \frac{p_i^2}{2m} + \sum_{n=1}^{K} \frac{P_n^2}{2M_n} + \frac{1}{2} \sum_{i,j=1,i\neq j}^{N} \frac{e^2}{|\mathbf{r}_i - \mathbf{r}_j|} - \sum_{i=1}^{N} \sum_{n=1}^{K} \frac{Z_n e^2}{|\mathbf{r}_i - \mathbf{R}_n|} + \frac{1}{2} \sum_{n,m=1,n\neq m}^{K} \frac{Z_n Z_m e^2}{|\mathbf{R}_n - \mathbf{R}_m|}, \tag{5}$$

with p_i the momentum of electron i, m its mass, and $\mathbf{r}_i$ its position vector; and for the nuclei the P_n the momentum of nucleus n, M_n its mass, $\mathbf{R}_n$ its position vector and finally Z_n its atomic number. In this equation, the first part describes the kinetic energy of the electrons, the second part the kinetic energy of the nuclei, followed the repulsion between the electrons, the Coulomb attraction between electrons and nuclei, and finally the Coulomb repulsion between nuclei. [7]

Several important approximations must be made in order to simplify a many-body problem. Two independent particle models will be discussed in this chapter, namely the Hartree-Fock theory and the Density Functional Theory.

2.2.1 The Born-Oppenheimer Approximation and the Independent Particle Model

The Born-Oppenheimer (BO) approximation is the assumption that the nuclei stand still, since the electrons move so rapidly that the motion of the nuclei, which are much heavier, can be neglected. The BO Hamiltonian for the electrons reads:

$$H_{\mathrm{BO}} = \sum_{i=1}^{N} \frac{p_i^2}{2m} + \frac{1}{2} \sum_{i,j=1,i\neq j}^{N} \frac{e^2}{|\mathbf{r}_i - \mathbf{r}_j|} - \sum_{i=1}^{N} \sum_{n=1}^{K} \frac{Z_n e^2}{|\mathbf{r}_i - \mathbf{R}_n|} + C. \tag{6}$$

Compared to the complete many-body Hamiltonian, this equation is much simpler. The constant C comes from the last term in eq. (5) which is the Coulomb repulsion between the nuclei.

Another assumption, called the Independent Particle Model, is that the interaction of the particles is incorporated in an average potential field due to both the nuclei and the other electrons. After these two assumptions, eq. (5) reduces to the following equation:

$$H_{IP} = \sum_{i=1}^{N} \left[\frac{p_i^2}{2m} + V(\mathbf{r}_i) \right]. \tag{7}$$

This equation may look less complex, yet the difficulty resides in the term $V(\mathbf{r}_i)$ which not only depends on the positions of the nuclei $\mathbf{R}_i$, but also on either the occupied eigenstates (Hartree-Fock) or on the electron density (Density Functional Theory). This means that the orbitals must be determined self-consistently. [7][8]

2.2.2 Hartree-Fock Theory

The Hartree-Fock theory assumes that the wave function of the many-body problem can be approximated by a single Slater determinant (for fermions) which is the exact solution for a problem of non-interacting electrons. The wave function for N particles with the variable $\mathbf{x}_i = (\mathbf{r}_i, s_i)$ representing the position vector and spin, respectively, then takes the following form:

$$\Psi_{\mathrm{AS}}(\mathbf{x}_1, ..., \mathbf{x}_N) = \frac{1}{\sqrt{N!}} \begin{vmatrix} \psi_1(\mathbf{x}_1) & ... & \psi_N(\mathbf{x}_1) \\ \vdots & \vdots & \vdots \\ \psi_1(\mathbf{x}_N) & ... & \psi_N(\mathbf{x}_N) \end{vmatrix}. \tag{8}$$

The wave function is then automatically anti-symmetric, a property which is required for fermions.

In a variational procedure, the single-particle orbitals are varied in order to minimize the expectation value for the energy, which is given as:

$$\langle E \rangle = \langle \Psi_{\mathrm{AS}} | \, H \, | \Psi_{\mathrm{AS}} \rangle \,, \tag{9}$$

under the condition that the orbitals $\psi_i(x)$ remain orthonormal. This procedure eventually leads to the Hartree-Fock equation:

$$\mathscr{F}\psi_k = \epsilon_k \psi_k, \tag{10}$$

with

$$\mathscr{F}\psi_k = \left[-\frac{1}{2}\nabla^2 - \sum_n \frac{Z_n}{|\mathbf{r}-\mathbf{R}_n|} \right] \psi_k(\mathbf{x}) + \sum_{l=1}^{N} \int |\psi_l(\mathbf{x}')|^2 \frac{1}{|\mathbf{r}-\mathbf{r}'|} \psi_k(\mathbf{x}) \, dx' - \sum_{l=1}^{N} \int \psi_l^*(\mathbf{x}') \frac{1}{|\mathbf{r}-\mathbf{r}'|} \psi_k(\mathbf{x}') \psi_l(\mathbf{x}) \, dx'. \tag{11}$$

Here, $\mathscr{F}$ is the so-called Fock operator. In this equation, the first term is the kinetic energy and the second is the electrostatic interaction between the electrons and nuclei. The next line contains the so-called Hartree potential, which is the electrostatic energy of the electrons in the field generated by the total electron density. The last line contains the exchange energy.
This equation is nonlinear, thus it must be solved by an iterative procedure to obtain self-consistency: the set of orbitals that give rise to the same set after solving eq. (11) are called the self-consistent orbitals. The self-consistent procedure starts with a first estimate of the orbitals, and successive iterations are performed with new orbitals until the self-consistency condition is reached.

The anti-symmetry of the electronic wave functions is exactly incorporated in this theory, and therefore there is no self-interaction: the Hartree potential term includes self-interaction (when $l = k$ in the summation) but the exchange energy term cancels it precisely when again $l = k$. [7][8][9]

2.2.3 Density Functional Theory

While the Hartree-Fock method is based on complicated many-electron wave functions, the Density Functional Theory (DFT) is based on the electron density instead. This has as great advantage that the electron density can be described by one or two (if spin is included) functions depending on the spatial coordinates and is therefore a lot easier to handle compared to the N single particle wave functions.

The Hohenberg-Kohn theorems form the basis of DFT and relate to any system consisting of electrons which are moving under influence of an exchange correlation potential. The theorems are stated as follows: [10]

1. The exchange correlation potential, and hence the total energy, is a unique functional of the electron density $n(\mathbf{r})$
2. There exists an exchange correlation potential for which the ground state energy and density are exact.

These theorems lead, after some manipulations, to the Kohn-Sham Hamiltonian, which reads:

$$H_{\mathrm{KS}} = -\frac{1}{2}\nabla^2 - \sum_n \frac{Z_n}{|\mathbf{r}-\mathbf{R}_n|} + \int n(\mathbf{r}') \frac{1}{|\mathbf{r}-\mathbf{r}'|} d^3r' + V_{\mathrm{xc}}[n](\mathbf{r}). \tag{12}$$

Here, $n(\mathbf{r})$ is the electron density, which is constructed from the Kohn-Sham orbitals, $H_{\mathrm{KS}}\psi_k(\mathbf{r}) = \epsilon_k \psi_k(\mathbf{r})$, via:

$$n(\mathbf{r}) = \sum_{k_{occ}} |\psi_k(\mathbf{r})|^2, \tag{13}$$

where the sum is over the lowest N (the occupied) orbitals. The first term in eq. (12) is the kinetic energy, the second is the external energy. The third term is the Hartree potential, which is the electrostatic energy of the electrons in the field generated by the total electron density. The last term is the exchange-correlation potential.

In the equation for the Kohn-Sham Hamiltonian, the form of the exchange-correlation potential $V_{\text{xc}}[n](\mathbf{r})$ is not known. However, there exists a potential for which the ground state energy and density are exact, according to the Hohenberg-Kohn theorems. Approximations to it are for example the Local Density Approximation (LDA) or the Generalised Gradients Approximations (GGA's). The LDA is the simplest form of the potential and is exact for an homogeneous electron gas. The GGA's work better when the electron density has strong spatial variation. The LDA potential at position $\mathbf{r}$ only depends on the density at that position; in the GGA's, the potential is also influenced is by the variation in the density.

The problem of the DFT is the presence of self-interacting terms due to the Hartree potential. In the HF theory, these terms were not present as they were compensated. In order to get rid of this problem in DFT, the HF exchange term can be included in the exchange-correlation potential. This is done in the so-called 'hybrid functionals'. These, however, are very time-consuming. [8][11]

2.2.4 Green's Functions

In this paragraph, the mathematical concept of Green's functions will be discussed. These functions completely describe the state of a quantum-mechanical system and enable us to describe systems which are coupled to environments, in contrast to using the eigenfunctions and eigenvalues of the Hamiltonian that can only be obtained for isolated systems. First the equilibrium Green's functions are discussed, and then the extension to non-equilibrium situations will take place.

The definition of the Green's function $G(z)$ with $z \in \mathbb{C}$ of a closed system described by Hamiltonian H is as follows:

$$G(z) = \frac{1}{z\mathbb{1} - H}, \tag{14}$$

where $\mathbb{1}$ is a unit operator. For a closed system, the Hamiltonian is Hermitian.

The eigenfunctions of the Hamiltonian are $|\psi_n\rangle$. Since the unit operator can be written as $\mathbb{1} = \sum_n |\psi_n\rangle\langle\psi_n|$ and the Schrödinger equation $H|\psi_n\rangle = E_n|\psi_n\rangle$ holds, the Green's function can be expanded in eigenfunctions of the Hamiltoninan:

$$G(z) = \sum_n |\psi_n\rangle \frac{1}{z - E_n} \langle\psi_n|. \tag{15}$$

In this equation, z can be any complex number. If z is chosen to be close to, but above the real axis (i.e. z is a positive imaginary number), the so-called retarded Green's function is obtained:

$$G^R(\epsilon) = \lim_{\eta \downarrow 0} \frac{1}{\epsilon\mathbb{1} - H + i\eta}, \tag{16}$$

where ϵ is the real part of z and $i\eta$ the imaginary part. From the retarded Green's function, the Density of States, or DOS, of a system can be obtained. The imaginary part of the retarded Green's function can be derived by using complex function theory which yields:

$$\text{Im}\left(G^R(\epsilon)\right) = -\pi \sum_n |\psi_n\rangle \delta(\epsilon - E_n) \langle\psi_n|. \tag{17}$$

By taking the trace of this, we obtain the DOS:

$$\text{DOS}(E) = -\frac{1}{\pi} \text{Tr}\left(\text{Im}\left(G^R(E)\right)\right). \tag{18}$$

In this research, we deal with systems coupled to environments, e.g. a molecule coupled to a lead. This means the Hamiltonian is no longer Hermitian, so the Green's function has to be extended to a non-equilibrium situation. There it is assumed that the equation (18) remains valid in the non-equilibrium

regime.

As an example, we consider an atom near a bulk contact, where the atom has a single energy level E_a. The full Hamiltonian of this system is $H = H_B + H_A + H_T$, where the first part is the bulk Hamiltonian, the second part the Hamiltonian of the atom and the third part the Hamiltonian of the coupling between the atom and the bulk contact. In matrix form:

$$H = \begin{pmatrix} H_A & -\tau \\ -\tau^\dagger & H_B \end{pmatrix}. \tag{19}$$

Here, the H_A and H_B are sub-matrices and τ is the coupling between atom and bulk. The Green's function of this system can also be written in matrix form:

$$G(z) = \begin{pmatrix} G_A & A^\dagger \\ A & G_B \end{pmatrix}, \tag{20}$$

where the sub-matrices all depend on z.

The Green's function satisfies equation (14) so we can write:

$$\begin{pmatrix} z - H_A & -\tau \\ -\tau^\dagger & z - H_B \end{pmatrix} \begin{pmatrix} G_A & A^\dagger \\ A & G_B \end{pmatrix} = \begin{pmatrix} \mathbb{1}_A & 0 \\ 0 & \mathbb{1}_B \end{pmatrix}. \tag{21}$$

When equations for the upper and lower left block are extracted and solved,

$$(z - H_A)G_A - \tau A = \mathbb{1}_A \tag{22}$$

$$-\tau^\dagger G_A + (z - H_B)A = 0, \tag{23}$$

we obtain as Green's function for the atom the following equation:

$$G_A(z) = \frac{1}{z\mathbb{1}_A - H_A - \Sigma}, \tag{24}$$

where

$$\Sigma = \tau g_B \tau^\dagger \tag{25}$$

and

$$g_B = \frac{1}{z\mathbb{1}_B - H_B}, \tag{26}$$

e.g. the Green's function of the environment. The Σ is called the self-energy, which captures the effect of the environment on the atom - our system: the real part of the self-energy shifts the discrete energy levels of our system and the imaginary part of it broadens the levels into a Lorentzian peak. [12][8][13]

2.3 Chiral Induced Spin-Selectivity

In this chapter, the physical phenomenon of chiral induced spin-selectivity (CISS) will be illustrated. Shortly stated, CISS is the spin polarization that occurs when an electric current passes through a chiral molecule.

2.3.1 Chiral molecules

A classic example of chirality are the human hands: our hands are non-superimposable mirror images of each other, meaning that the mirror image of one of the hands does not overlap the original. When speaking of chirality in chemistry, molecules which support two distinct geometries are meant: the original molecule and its mirror image which cannot be brought to coincide with the original. The original molecule and its mirror image are called enantiomers. The following image may clarify the difference between chiral and achiral molecules.

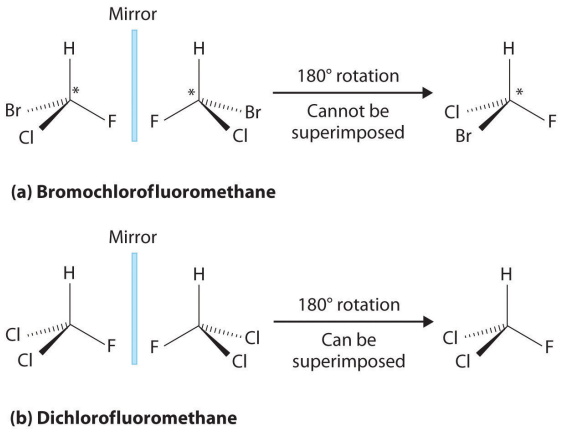

Figure 1: A chiral and an achiral molecule. Molecule (a) is an example of a chiral molecule. The mirror image of the molecule cannot be superimposed on the original molecule. The mirror image of molecule (b), on the other hand, can be superimposed on the original, thus is an achiral molecule. [14]

An important property of chiral molecules is that a pair of enantiomers rotate plane-polarized light (light waves that are vibrating in the same, parallel, direction) to an equal degree, but in the opposite direction. Molecules that influence the polarization of light are called optically active.

2.3.2 Helicene

An example of a chiral molecules are so-called helicenes. These are helically-shaped molecules consisting of benzene rings or other aromatics; n-helicene is a molecule with n rings. See the following image for an overview.

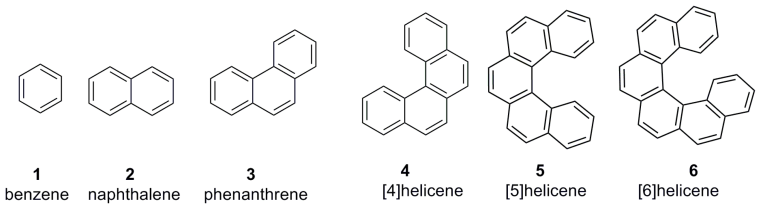

Figure 2: An overview of the construction of 4,5 and 6-helicene from benzene rings. [15]

In this research, a thiolated 4-helicene molecule is used in the model, meaning that the outermost H-atoms are replaced by S-atoms, to ensure a good bond with the Au-atoms from the contacts.

2.3.3 Polarization

Two types of polarization are described here: in addition to the well-known polarization of photons by chiral molecules, the electron spin can also be polarized by chiral molecules, a phenomenon which is known as CISS.

Experiments on the rotation of light polarization by chiral molecules start off with a light source, where the waves vibrate in all directions. A filter with small slits, called the polarizer, polarizes the light waves, so only plane-polarized light comes out. This plane-polarized light travels through a tube filled with an optically active sample, which rotates the plane of polarized light. This can be explained by the fact that the speed of light in this sample is different for right circularly polarized and left circularly polarized light. By using an analyzer, which is a rotatable filter, the rotation angle can be observed. See the following image for an overview.

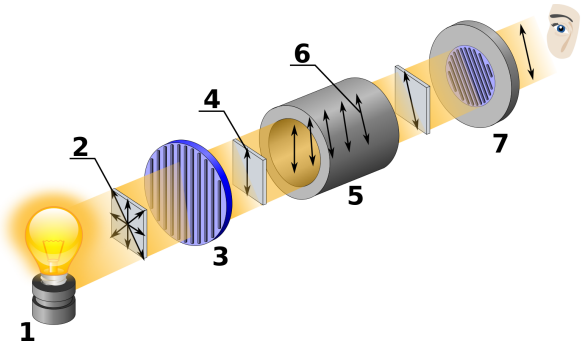

Figure 3: A classic set-up for measuring the rotation angle, with **1**) the light source, **2**) unpolarized light waves, **3**) the polarizer, **4**) plane-polarized light waves, **5**) tube filled with optically active sample, **6**) the rotation of the plane of the polarized light and **7**) the rotatable analyzer. [16]

As explained in the previous section, enantiomers rotate the plane-polarized light to an equal degree, but in opposite directions: when the rotation angle is positive, the molecule is called dextrorotatory; when the rotation angle is negative, the molecule is called levorotatory.

Chiral molecules do not only rotate the polarization photon beams, but also rotate electron spin in a similar manner. [17]
Now we take a helix-shaped molecule as an example. This molecule has a chiral electrostatic potential. As an electron moves along the axis of the helical charge distribution, it experiences a magnetic field **B**:

$$\mathbf{B} = \frac{\mathbf{v}}{c^2} \times \mathbf{E}_{\text{chiral}}. \tag{27}$$

Here, **v** is the velocity of the moving electron, c is the speed of light and $\mathbf{E}_{chiral}$ is the electric field acting on the electron while it moves through the chiral molecule. This electric field is generated by the nuclei and electrons that make up the chiral molecule, and perhaps a bias field when the molecule is placed in between two contacts. [1]
The magnetic moment μ of the electron, which is due to its spin, will be influenced by this magnetic field. Depending on the handedness of the helix, the ground state of the electron is either the spin-up or the spin-down state. Therefore, spin filtering takes place: one of the two spin-states is favored over the other.

2.3.4 Examples

The effect of CISS has been studied extensively in experiments. Two of these studies will be described in this paragraph, as an example.

Photoelectron transmission measurements through an absorbed monolayer of double stranded DNA (ds-DNA) molecules on a gold substrate were done by Göhler et al. [3] When the substrate is irradiated with

X-rays, photoelectrons are ejected from the metal and then pass through monolayer. A Mott polarimeter measures the spin polarization of the transmitted photoelectrons as it separates the electron beam into spin-up and spin-down components. Spin polarizations exceeding 60% at room temperature were measured, where the spin polarization is defined by the following equation:

$$P = \frac{j_\uparrow - j_\downarrow}{j_\uparrow + j_\downarrow}, \tag{28}$$

where $j_{\uparrow,\downarrow}$ are the currents associated with each spin. It was also found that spin polarization occurs when the X-rays were not polarized, and that it depended on both the length of the DNA in the monolayer and its organization.

Conductance measurements through an adsorbed monolayer of double-stranded DNA (dsDNA) oligomers were done by Xie et al. [2]. The experimental setup consists of a permanent magnet, on which a nickel substrate resides. The permanent magnet determines whether only spin-up or spin-down electrons pass through the system. The nickel surface functions as the bottom electrode. The dsDNA oligomers are bound on one end to the nickel surface. The outer ends are chemically bound to gold nanoparticles, which make up the top electrode. An Atomic Force Microscope (AFM) is used to measure the current between the nickel substrate and the tip of the AFM. The electric potential was varied between -3 to +3 V. See the following image for an overview of the setup.

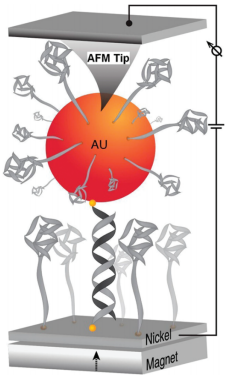

Figure 4: The experimental setup used in reference [2].

The result of the experiments were that the conductance is significantly different for the two spin orientations. The molecule's conductance depended on both the orientation of the permanent magnet and on the length of the dsDNA oligomers.

3 Models and Results

In this research, a conductance measurement through a thiolated 4-helicene molecule placed between two Au-contacts is simulated by means of the Amsterdam Density Functional (ADF) program from the Software for Chemistry and Material (SCM) [18]. The simulation takes place in two main steps. In the first step, the geometry of both the helicene molecule and the Au-contacts is optimized. This geometry optimization is done in two different ways. Secondly, a transport calculation is performed on both the geometrically optimized systems, and on the non-optimized system: the density of states (DOS) and the electron transmission of the molecule are calculated. The results of the three transport calculations are then discussed and compared.

3.1 Geometry Optimization

3.1.1 Input Coordinates

Before a geometry optimization can be performed, a rough estimate of the coordinates of the system must be found. The Graphical User Interface (GUI) of SCM provides an excellent tool for this.

The geometry of the Au-contacts is based on the provided examples *green_BDT* and *green_Au* [19][20]. The coordinates of the gold are copied from these scripts and placed in a xyz-file which is loaded into the GUI. There is chosen for gold as the material for the contacts since both the DOS and the transmission of gold are relatively constant around the Fermi energy (the chemical potential at temperature $T = 0$), which is approximately -2.0 Hartree. [21][20].

The geometry of the helicene molecule is based on one of the scripts from M. Rebergen's Master Thesis [17]. This helicene molecule is convenient for this research as it clearly shows a helical shape, indicating the molecule is chiral, and it contains S-atoms, which ensures a proper binding with the gold contacts. Again, the coordinates are copied and placed in a xyz-file which is also loaded in the GUI.

In the GUI, the molecule is both shifted and rotated and the contacts are shifted in only the x-direction, until the molecule fits well between the contacts. See also the following figure:

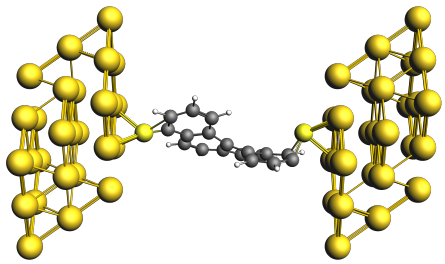

Figure 5: System '1: the thiolated 4-helicene molecule between two gold contacts in pre-optimizated configuration. [18]

Then, by exporting the coordinates, a rough estimate of the coordinates of the entire system is found.

3.1.2 Optimization

The geometry optimization is done in two different ways. In the first method, the geometry of the system is optimized under the constraints that the y- and z-coordinates of the Au atoms are fixed, and the thiolated helicene molecule is free to move. The second method uses a different approach: the atoms of the contacts are completely frozen on their initial positions, and the thiolated helicene molecule is free to move. During optimization, the atomic coordinates are varied in an attempt to find an energy minimum [22]. This is an iterative procedure; when the computation has converged, the coordinates of the last cycle are used as output to construct the images as shown in the following two sections.

Method 1 After the first geometry optimization, the system has the configuration as shown in figure 6. This figure shows that indeed the atoms of the gold contacts could only move in the x-direction; there is no question of rotations or translations of the contacts. However, the contacts do not have a crystalline structure anymore; the distances between the gold atoms within the contacts are not the same. Since the transport calculation only works with a crystalline structure of the contacts, the contacts are replaced with the original contacts. The configuration of the system after this replacement is shown in figure 7. This configuration will be referred to as System 2.

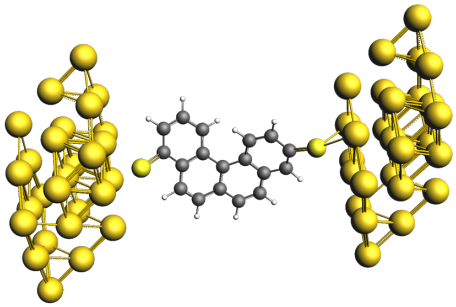

Figure 6: The thiolated 4-helicene molecule between two gold contacts in optimized configuration. The gold contacts do not have a crystalline structure. [18]

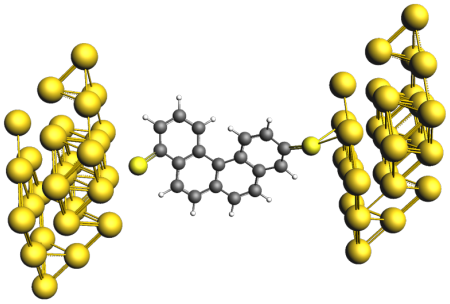

Figure 7: System 2: The thiolated 4-helicene molecule between two gold contacts in optimized configuration, with the gold contacts replaced by the ones in the pre-optimized configuration. [18]

The script of this geometry optimization is included in the Appendix A.1.

Method 2 In this second approach the system is optimized under the constraints that the two contacts are frozen to their initial positions. The lattice structure of the contacts will therefore be retained, ensuring a feasible transport calculation. The system in optimized configuration is shown in the following figure. This configuration will be referred to as System 3.

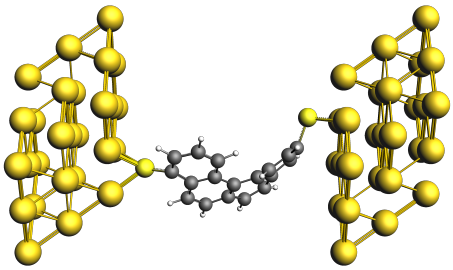

Figure 8: System 3: The thiolated 4-helicene molecule between two gold contacts in optimized configuration. [18]

The script of this geometry optimization is included in the Appendix A.2.

3.2 Transport Calculation

In this part, the DOS, see eq. (18), and the electron transmission of the 4-helicene molecule between the gold electrodes is calculated by using the ADF program *green* [18]. The transport calculation consists of two main parts: first, the effect of the contacts on the molecule is calculated, which is contained in the self-energies of the contacts, see eq. (25), and secondly the DOS and electron transmission of the molecule are calculated. This is done for the three configurations of the system: the non-optimized system, the optimized system via method 1 and the optimized via method 2.

3.2.1 Self-energy Calculation

As previously mentioned, the gold contacts are based on the contacts from *green_BDT* and *green_Au*, with only 3 layers of 3x3 = 9 gold atoms, so in total 27 atoms each. Ideally, the contacts are semi-infinite. Since one cannot model systems of infinite size, approximations are made: the contacts consist of so many layers that the atoms on one side are not influenced by whatever is attached to the other side. The calculation of the self-energies of the contacts is therefore a bulk calculation: one needs to ensure that the Hamiltonians of the contacts are bulk Hamiltonians. [23]

Since the self-energies of the contacts are independent of both the type of molecule and its coordinates that is put between them, the result obtained can be reused when a change in the configuration of the molecule takes place.

The starting point of the calculation of the self-energy of the gold contacts is the following geometry:

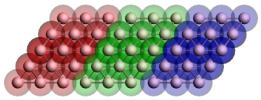

Figure 9: The geometry of a single gold contact used in the calculation of the self-energy. [20]

In this figure, each colour indicates a different principal layer, being FLTR the left-, the bulk- and the right layer. Each principal layer in turn consists of three atomic layers. Both the construction of this geometry and the self-energy calculation is covered in the script *Self-Energy Calculation* provided in the Appendix B [20]. This script consists of 4 parts, which are described as follows:

Part 1: Atomic Layer Construction The geometry of an atomic layer is build up atom by atom by using the already existing files *Au.5p* and *Au.5p.dirac*. An atomic layer contains 3x3 = 9 gold atoms. Since relativistic effects are relevant for gold atoms, the Relativistic Scalar ZORA (Zero Order Regular Approximation) is used. The configuration of the atoms in this layer is such that both a top-, bridge-, and hollow-site binding with another atom - such as a sulfur atom - is possible. See also the following figure:

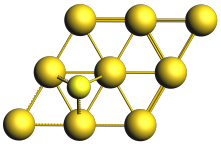

Figure 10: A sulphur atom adsorbed on the hollow site of the atomic layer. [18]

The hollow-site binding is the most favourable one as it is the most stable as compared to the other bindings [24].

Part 2: Principal Layer Construction Next, a principal layer of gold is build up by stacking three atomic layers. The principal layer is displayed in the following image:

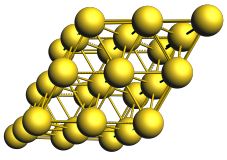

Figure 11: The principle layer as constructed in part 4. [18]

In this part of the script, the file called *layer.t21* is created.

Part 3: Bulk Layer Construction Finally, three principal layers of gold are stacked in order to acquire the geometry displayed in figure (9). Now, the *bulk.t21*-file is created, which is the input file for the self-energy calculation.

Part 4: Self-Energy Calculation By using a green calculation, the self-energy of both the left and the right contact is computed with the key called *SURFACE*. This is done for every energy for which the DOS and transmission have to be calculated; the energy range is given by the key *EPS*. The calculation of the self-energy of the left contact uses the center and the right fragment. The calculation of the self-energy of the right contact uses the center and the left fragment. The output are two files, *left.kf* and *right.kf*, being the self-energy of the left contact and of the right contact, respectively.

3.2.2 DOS and Transmission Calculation

Calculation Now that the self-energies of the contacts are obtained, the DOS and transmission of the molecule can be calculated. The script for this calculation is included in Appendix C and is based on the script of the *green_BDT* example [19]. For all three configurations of the system the same script is used, but with various atom coordinates of course. It is based on the non-self-consistent Green's function method, which is an approximation of the NEGF method (see Chapter 2.2.4).

First, the isolated molecule with the xyz-coordinates as obtained in the geometry optimization is constructed by performing a single-point calculation[2], creating a *molecule.t21*-file. Next, the molecule is sandwiched between the gold contacts, by using the fragment of the principal layer as obtained in the self-energy calculation of the contacts (the *layer.t21*-file). The so-called extended molecule is created, again by performing a single-point calculation. This output is placed in the *fock.t21*-file. From the self-energies of the contacts and the *fock.t21*-file, the DOS and transmission is calculated by the ADF program *green*.

Results The results of the DOS and transmission calculations for one of the two spin orientations are shown in figure 12 and 13, respectively. Since the results of the two spin states were exact copies, the DOS and transmission of the other spin orientation are not presented. The figures were obtained by using the program MATLAB [25]. In the DOS figure, the DOS, $D(E)$, is plotted against the energy E. In the transmission figure, the transmission, $T(E)$, is plotted against the energy as well. System 1 corresponds to the non-optimized geometry, system 2 corresponds to the optimized geometry via the first method, and system 3 corresponds to the optimized geometry via the second method.

The DOS graphs of the three systems do not show much difference with respect to each other. The density of states is small and approximately constant between -0.26 Hartree, so just below the Fermi energy of the contacts, and -0.08 Hartree, so just above this energy. Below around -0.26 Hartree, the density of states forms a broad peak. At around -0.06 Hartree a sharper, but smaller, peak is visible.

The transmission figure displays that the three systems show different transmission behaviour. The non-optimized geometry (system 1) deviates the most from the other two geometries, which are both optimized. Around the Fermi energy of the contacts, the transmission is close to zero and almost constant for system 2 and 3. For system 1, the transmission still shows fluctuation above zero around the Fermi energy of the contacts.

[2] ADF provides different run types, one of them being the SinglePoint: the Self Consistent Field solution is computed for the input geometry [22]. Examples of self-consistent calculations are the DFT and HF theory as discussed in the chapter Theory.

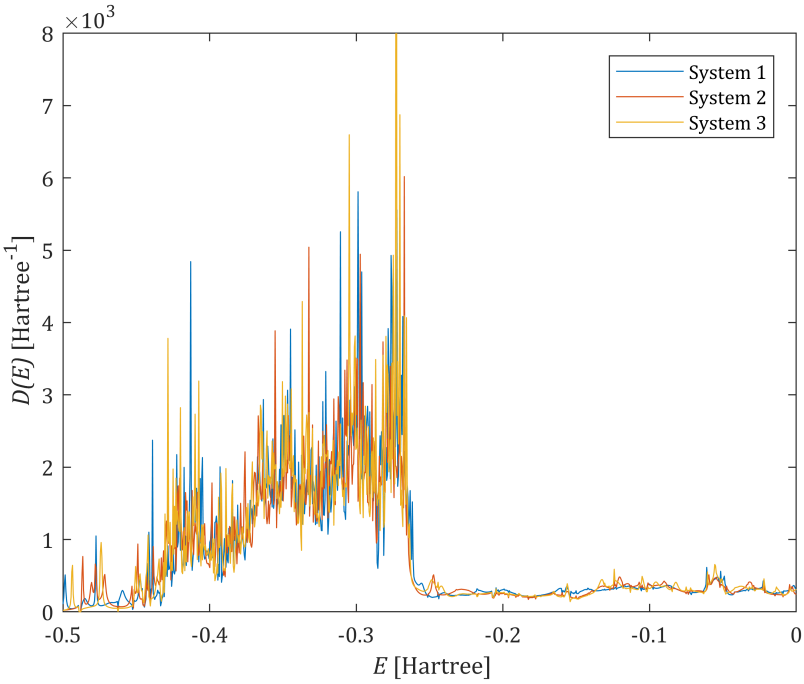

Figure 12: The Density of States $D(E)$ [Hartree^{-1}] plotted against the energy [Hartree] for the three different systems. System 1 corresponds to the non-optimized geometry, system 2 to the first optimized geometry and system 2 to the second optimized geometry. Graph created in MATLAB [25].

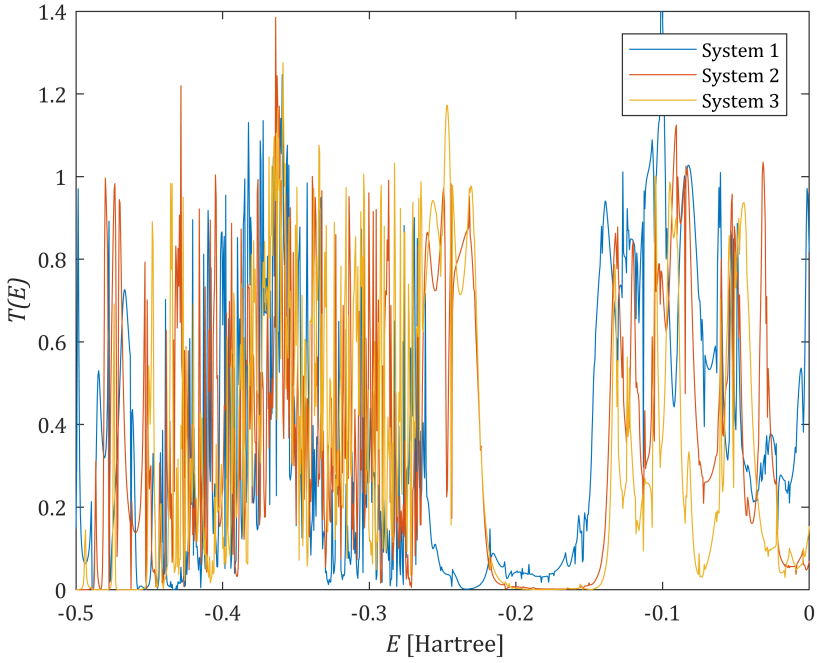

Figure 13: The transmission $T(E)$ [-] plotted against the energy [Hartree] for the three different systems. System 1 corresponds to the non-optimized geometry, system 2 to the first optimized geometry and system 2 to the second optimized geometry. Graph created in MATLAB [25].

4 Conclusions and Discussion

In the master thesis of Rebergen it has been demonstrated that spin polarization occurred in the models of a thiolated 4-helicene molecule between two golden contacts [17]. However, in our results we could not demonstrate this polarization. Both the density of states and the transmission for the two different spin orientations were found to be exact copies of each other. This can be explained by the fact that in the transport calculation, nothing was specified about the restriction on the spin, and that the relativistic scalar ZORA was used instead of the relativistic spin-orbit ZORA [personal communication Jos Thijssen]. Furthermore the calculations had long run times since we did not use the so-called Wide Band Limit (see [26]) in order to speed them up.

The density of states of the three different systems is very similar; there is little variation visible in the three graphs. The Highest Occupied Molecular Orbital (HOMO) combined with lower orbitals form a broad peak in the density of states graph. The HOMO is situated just below the Fermi energy of the contacts, at around -0.26 Hartree, which is consistent with literature [27]. The Lowest Unoccupied Molecular Orbital (LUMO) is also visible in the graphs for the density of states: it is the sharper and smaller peak situated above the Fermi energy of the contacts, at around -0.06 Hartree.

The transmission of the three systems shows greater variation. Especially the difference between the non-optimized geometry and the two optimized ones stands out. Around the Fermi energy of the contacts, the transmission is close to zero and approximately constant for the optimized systems. This is consistent with the density of states which is almost zero around the Fermi energy; when no or few electrons are present around a certain energy level, the electron transmission automatically drops as well. For the non-optimized geometry, the transmission still shows fluctuations above zero around the Fermi energy of the contacts. This indicates the impurities in the non-optimized system, and the improvement through the performed geometry optimizations.

In conclusion, for further research, it is recommended to apply the so-called Wide Band Limit in order to speed up the calculations. To investigate the effect of spin polarization in chiral molecules, one should perform a spin-unrestricted transport calculation by using the key *UNRESTRICTED*, as well as using the spin-orbit ZORA instead of the scalar ZORA.

A Geometry Optimization Scripts

A.1 Method 1

```
$ADFBIN/adf <<eor
Title y-z-Constraints_Helicene

# There is no symmetry in the system
SYMMETRY NOSYM

# Configuration of the system; coordinates in xyz-format, unit Angstrom.
ATOMS
```

1	Au	−11.41117700	−6.66261200	0.00000000
2	Au	−11.41117800	−4.16413300	−1.44249800
3	Au	−11.41117800	−4.16413300	1.44249800
4	Au	−11.41117800	−1.66565300	−2.88499600
5	Au	−11.41117800	−1.66565300	0.00000000
6	Au	−11.41117800	−1.66565300	2.88499600
7	Au	−11.41117800	0.83282600	−1.44249800
8	Au	−11.41117800	0.83282600	1.44249800
9	Au	−11.41117800	3.33130600	0.00000000
10	Au	−9.05558900	−4.99695900	0.00000000
11	Au	−9.05558900	−2.49848000	−1.44249800
12	Au	−9.05558900	−2.49848000	1.44249800
13	Au	−9.05558900	0.00000000	−2.88499600
14	Au	−9.05558900	0.00000000	0.00000000
15	Au	−9.05558900	0.00000000	2.88499600
16	Au	−9.05558900	2.49848000	−1.44249800
17	Au	−9.05558900	2.49848000	1.44249800
18	Au	−9.05558900	4.99695900	0.00000000
19	Au	−6.70000000	−3.33130600	0.00000000
20	Au	−6.70000000	−0.83282600	−1.44249800
21	Au	−6.70000000	−0.83282600	1.44249800
22	Au	−6.70000000	1.66565300	−2.88499600
23	Au	−6.70000000	1.66565300	0.00000000
24	Au	−6.70000000	1.66565300	2.88499600
25	Au	−6.70000000	4.16413300	−1.44249800
26	Au	−6.70000000	4.16413300	1.44249800
27	Au	−6.70000100	6.66261200	0.00000000
28	Au	11.41117800	4.16413300	1.44249800
29	Au	11.41117800	4.16413300	−1.44249800
30	Au	11.41117700	6.66261200	0.00000000
31	Au	11.41117800	1.66565300	2.88499600
32	Au	11.41117800	−0.83282600	−1.44249800
33	Au	9.05558900	4.99695900	0.00000000
34	Au	11.41117800	1.66565300	−2.88499600
35	Au	11.41117800	−0.83282600	1.44249800
36	Au	11.41117800	1.66565300	0.00000000
37	Au	11.41117800	−3.33130600	0.00000000
38	S	−4.70000000	0.00000000	0.00000000
39	S	4.70000000	0.00000000	0.00000000
40	Au	6.70000100	−6.66261200	0.00000000
41	Au	6.70000000	−4.16413300	−1.44249800
42	Au	6.70000000	−4.16413300	1.44249800

43	Au	6.70000000	−1.66565300	−2.88499600
44	Au	6.70000000	−1.66565300	0.00000000
45	Au	6.70000000	−1.66565300	2.88499600
46	Au	6.70000000	0.83282600	−1.44249800
47	Au	6.70000000	0.83282600	1.44249800
48	Au	6.70000000	3.33130600	0.00000000
49	Au	9.05558900	−4.99695900	0.00000000
50	Au	9.05558900	−2.49848000	−1.44249800
51	Au	9.05558900	−2.49848000	1.44249800
52	Au	9.05558900	0.00000000	−2.88499600
53	Au	9.05558900	0.00000000	0.00000000
54	Au	9.05558900	0.00000000	2.88499600
55	Au	9.05558900	2.49848000	−1.44249800
56	Au	9.05558900	2.49848000	1.44249800
57	C	3.98953912	−1.57283209	0.46556843
58	C	3.84179542	−1.31486749	−0.86926863
59	C	2.86980455	−1.75249889	1.27011413
60	C	2.55422697	−1.25444789	−1.40860089
61	C	1.60495816	−1.59813549	0.77354805
62	C	1.43006145	−1.15498419	−0.53783399
63	C	2.32633965	−1.38639749	−2.79496668
64	C	1.07379568	−1.33648859	−3.29762650
65	C	0.18254797	−0.69807759	−1.11826255
66	C	−0.03745295	−1.04477829	−2.47659288
67	C	−0.88460388	0.00915171	−0.44371432
68	C	−0.70448321	0.85822241	0.65820930
69	C	−1.78604267	1.30361751	1.35656767
70	C	−1.33731274	−1.01548009	−3.00769203
71	C	−2.20059157	−0.15766099	−0.94449996
72	C	−3.08367615	0.93548501	1.00062926
73	C	−2.39536074	−0.64609709	−2.24560618
74	C	−3.29478703	0.20446611	−0.14789025
75	H	0.28514938	1.16839221	0.96400214
76	H	4.71061388	−1.16675399	−1.49402462
77	H	3.00100497	−2.02587749	2.30810790
78	H	3.16356536	−1.53259479	−3.46154986
79	H	0.91849833	−1.52094629	−4.35156435
80	H	−1.63929661	1.95619161	2.20575600
81	H	−1.50293858	−1.29106249	−4.03981200
82	H	−3.39406067	−0.72582719	−2.64968388
83	H	−3.92607270	1.21683611	1.61512875
84	H	0.75639511	−1.82540739	1.40424856

END

Keep the y and z coordinates of the contacts frozen during optimization
CONSTRAINTS

COORD	1	2	−6.662612
COORD	2	2	−4.164133
COORD	3	2	−4.164133
COORD	4	2	−1.665653
COORD	5	2	−1.665653
COORD	6	2	−1.665653
COORD	7	2	0.832826

COORD	8	2	0.832826
COORD	9	2	3.331306
COORD	10	2	−4.996959
COORD	11	2	−2.49848
COORD	12	2	−2.49848
COORD	13	2	0.000000
COORD	14	2	0
COORD	15	2	0
COORD	16	2	2.49848
COORD	17	2	2.49848
COORD	18	2	4.996959
COORD	19	2	−3.331306
COORD	20	2	−0.832826
COORD	21	2	−0.832826
COORD	22	2	1.665653
COORD	23	2	1.665653
COORD	24	2	1.665653
COORD	25	2	4.164133
COORD	26	2	4.164133
COORD	27	2	6.662612
COORD	28	2	4.164133
COORD	29	2	4.164133
COORD	30	2	6.662612
COORD	31	2	1.665653
COORD	32	2	−0.832826
COORD	33	2	4.996959
COORD	34	2	1.665653
COORD	35	2	−0.832826
COORD	36	2	1.665653
COORD	37	2	−3.331306
COORD	38	2	0
COORD	39	2	0
COORD	40	2	−6.662612
COORD	41	2	−4.164133
COORD	42	2	−4.164133
COORD	43	2	−1.665653
COORD	44	2	−1.665653
COORD	45	2	−1.665653
COORD	46	2	0.832826
COORD	47	2	0.832826
COORD	48	2	3.331306
COORD	49	2	−4.996959
COORD	50	2	−2.49848
COORD	51	2	−2.49848
COORD	52	2	0
COORD	53	2	0
COORD	54	2	0
COORD	55	2	2.49848
COORD	56	2	2.49848
COORD	1	3	0
COORD	2	3	−1.442498
COORD	3	3	1.442498
COORD	4	3	−2.884996
COORD	5	3	0

```
COORD   6       3       2.884996
COORD   7       3       −1.442498
COORD   8       3       1.442498
COORD   9       3       0
COORD   10      3       0
COORD   11      3       −1.442498
COORD   12      3       1.442498
COORD   13      3       −2.884996
COORD   14      3       0
COORD   15      3       2.884996
COORD   16      3       −1.442498
COORD   17      3       1.442498
COORD   18      3       0
COORD   19      3       0
COORD   20      3       −1.442498
COORD   21      3       1.442498
COORD   22      3       −2.884996
COORD   23      3       0
COORD   24      3       2.884996
COORD   25      3       −1.442498
COORD   26      3       1.442498
COORD   27      3       0
COORD   28      3       1.442498
COORD   29      3       −1.442498
COORD   30      3       0
COORD   31      3       2.884996
COORD   32      3       −1.442498
COORD   33      3       0
COORD   34      3       −2.884996
COORD   35      3       1.442498
COORD   36      3       0
COORD   37      3       0
COORD   38      3       0
COORD   39      3       0
COORD   40      3       0
COORD   41      3       −1.442498
COORD   42      3       1.442498
COORD   43      3       −2.884996
COORD   44      3       0
COORD   45      3       2.884996
COORD   46      3       −1.442498
COORD   47      3       1.442498
COORD   48      3       0
COORD   49      3       0
COORD   50      3       −1.442498
COORD   51      3       1.442498
COORD   52      3       −2.884996
COORD   53      3       0
COORD   54      3       2.884996
COORD   55      3       −1.442498
COORD   56      3       1.442498

END
```

```
BASIS
  type DZ
END

Relativistic Scalar ZORA

#Exchange-Correlation potential approximated by the Local Density Approximation.
XC
        LDA VWN
END

# Initialize Cartesian geometry optimization
GEOMETRY
     Optim Cartesian
     Branch new
END

eor

rm TAPE21 logfile
```

A.2 Method 2

```
$ADFBIN/adf <<eor
Title x-y-z-Constraints_Helicene

# There is no symmetry in the system
SYMMETRY NOSYM

# Configuration of the sytem; coordinates in xyz-format, unit Angstrom.
ATOMS
```

1	Au	−11.4111770	−6.6626120	0.0000000
2	Au	−11.4111780	−4.1641330	−1.4424980
3	Au	−11.4111780	−4.1641330	1.4424980
4	Au	−11.4111780	−1.6656530	−2.8849960
5	Au	−11.4111780	−1.6656530	0.0000000
6	Au	−11.4111780	−1.6656530	2.8849960
7	Au	−11.4111780	0.8328260	−1.4424980
8	Au	−11.4111780	0.8328260	1.4424980
9	Au	−11.4111780	3.3313060	0.0000000
10	Au	−9.0555890	−4.9969590	0.0000000
11	Au	−9.0555890	−2.4984800	−1.4424980
12	Au	−9.0555890	−2.4984800	1.4424980
13	Au	−9.0555890	0.0000000	−2.8849960
14	Au	−9.0555890	0.0000000	0.0000000
15	Au	−9.0555890	0.0000000	2.8849960
16	Au	−9.0555890	2.4984800	−1.4424980
17	Au	−9.0555890	2.4984800	1.4424980
18	Au	−9.0555890	4.9969590	0.0000000
19	Au	−6.7000000	−3.3313060	0.0000000
20	Au	−6.7000000	−0.8328260	−1.4424980
21	Au	−6.7000000	−0.8328260	1.4424980
22	Au	−6.7000000	1.6656530	−2.8849960
23	Au	−6.7000000	1.6656530	0.0000000
24	Au	−6.7000000	1.6656530	2.8849960
25	Au	−6.7000000	4.1641330	−1.4424980
26	Au	−6.7000000	4.1641330	1.4424980
27	Au	−6.7000010	6.6626120	0.0000000
28	Au	11.4111780	4.1641330	1.4424980
29	Au	11.4111780	4.1641330	−1.4424980
30	Au	11.4111770	6.6626120	0.0000000
31	Au	11.4111780	1.6656530	2.8849960
32	Au	11.4111780	−0.8328260	−1.4424980
33	Au	9.0555890	4.9969590	0.0000000
34	Au	11.4111780	1.6656530	−2.8849960
35	Au	11.4111780	−0.8328260	1.4424980
36	Au	11.4111780	1.6656530	0.0000000
37	Au	11.4111780	−3.3313060	0.0000000
38	Au	6.7000010	−6.6626120	0.0000000
39	Au	6.7000000	−4.1641330	−1.4424980
40	Au	6.7000000	−4.1641330	1.4424980
41	Au	6.7000000	−1.6656530	−2.8849960
42	Au	6.7000000	−1.6656530	0.0000000
43	Au	6.7000000	−1.6656530	2.8849960
44	Au	6.7000000	0.8328260	−1.4424980

45	Au	6.7000000	0.8328260	1.4424980
46	Au	6.7000000	3.3313060	0.0000000
47	Au	9.0555890	−4.9969590	0.0000000
48	Au	9.0555890	−2.4984800	−1.4424980
49	Au	9.0555890	−2.4984800	1.4424980
50	Au	9.0555890	0.0000000	−2.8849960
51	Au	9.0555890	0.0000000	0.0000000
52	Au	9.0555890	0.0000000	2.8849960
53	Au	9.0555890	2.4984800	−1.4424980
54	Au	9.0555890	2.4984800	1.4424980
55	S	−4.7000000	0.0000000	0.0000000
56	S	4.7000000	0.0000000	0.0000000
57	C	3.9895391	−1.5728321	0.4655684
58	C	3.8417954	−1.3148675	−0.8692686
59	C	2.8698046	−1.7524989	1.2701141
60	C	2.5542270	−1.2544479	−1.4086009
61	C	1.6049582	−1.5981355	0.7735481
62	C	1.4300615	−1.1549842	−0.5378340
63	C	2.3263397	−1.3863975	−2.7949667
64	C	1.0737957	−1.3364886	−3.2976265
65	C	0.1825480	−0.6980776	−1.1182626
66	C	−0.0374530	−1.0447783	−2.4765929
67	C	−0.8846039	0.0091517	−0.4437143
68	C	−0.7044832	0.8582224	0.6582093
69	C	−1.7860427	1.3036175	1.3565677
70	C	−1.3373127	−1.0154801	−3.0076920
71	C	−2.2005916	−0.1576610	−0.9445000
72	C	−3.0836762	0.9354850	1.0006293
73	C	−2.3953607	−0.6460971	−2.2456062
74	C	−3.2947870	0.2044661	−0.1478903
75	H	0.2851494	1.1683922	0.9640021
76	H	4.7106139	−1.1667540	−1.4940246
77	H	3.0010050	−2.0258775	2.3081079
78	H	3.1635654	−1.5325948	−3.4615499
79	H	0.9184983	−1.5209463	−4.3515644
80	H	−1.6392966	1.9561916	2.2057560
81	H	−1.5029386	−1.2910625	−4.0398120
82	H	−3.3940607	−0.7258272	−2.6496839
83	H	−3.9260727	1.2168361	1.6151288
84	H	0.7563951	−1.8254074	1.4042486

END

Keep the x, y and z coordinates of the contacts the same.

CONSTRAINTS

ATOM	1	−11.4111770	−6.6626120	0.0000000
ATOM	2	−11.4111780	−4.1641330	−1.4424980
ATOM	3	−11.4111780	−4.1641330	1.4424980
ATOM	4	−11.4111780	−1.6656530	−2.8849960
ATOM	5	−11.4111780	−1.6656530	0.0000000
ATOM	6	−11.4111780	−1.6656530	2.8849960
ATOM	7	−11.4111780	0.8328260	−1.4424980
ATOM	8	−11.4111780	0.8328260	1.4424980
ATOM	9	−11.4111780	3.3313060	0.0000000
ATOM	10	−9.0555890	−4.9969590	0.0000000

```
    ATOM      11          -9.0555890      -2.4984800      -1.4424980
    ATOM      12          -9.0555890      -2.4984800       1.4424980
    ATOM      13          -9.0555890       0.0000000      -2.8849960
    ATOM      14          -9.0555890       0.0000000       0.0000000
    ATOM      15          -9.0555890       0.0000000       2.8849960
    ATOM      16          -9.0555890       2.4984800      -1.4424980
    ATOM      17          -9.0555890       2.4984800       1.4424980
    ATOM      18          -9.0555890       4.9969590       0.0000000
    ATOM      19          -6.7000000      -3.3313060       0.0000000
    ATOM      20          -6.7000000      -0.8328260      -1.4424980
    ATOM      21          -6.7000000      -0.8328260       1.4424980
    ATOM      22          -6.7000000       1.6656530      -2.8849960
    ATOM      23          -6.7000000       1.6656530       0.0000000
    ATOM      24          -6.7000000       1.6656530       2.8849960
    ATOM      25          -6.7000000       4.1641330      -1.4424980
    ATOM      26          -6.7000000       4.1641330       1.4424980
    ATOM      27          -6.7000010       6.6626120       0.0000000
    ATOM      28          11.4111780       4.1641330       1.4424980
    ATOM      29          11.4111780       4.1641330      -1.4424980
    ATOM      30          11.4111770       6.6626120       0.0000000
    ATOM      31          11.4111780       1.6656530       2.8849960
    ATOM      32          11.4111780      -0.8328260      -1.4424980
    ATOM      33           9.0555890       4.9969590       0.0000000
    ATOM      34          11.4111780       1.6656530      -2.8849960
    ATOM      35          11.4111780      -0.8328260       1.4424980
    ATOM      36          11.4111780       1.6656530       0.0000000
    ATOM      37          11.4111780      -3.3313060       0.0000000
    ATOM      38           6.7000010      -6.6626120       0.0000000
    ATOM      39           6.7000000      -4.1641330      -1.4424980
    ATOM      40           6.7000000      -4.1641330       1.4424980
    ATOM      41           6.7000000      -1.6656530      -2.8849960
    ATOM      42           6.7000000      -1.6656530       0.0000000
    ATOM      43           6.7000000      -1.6656530       2.8849960
    ATOM      44           6.7000000       0.8328260      -1.4424980
    ATOM      45           6.7000000       0.8328260       1.4424980
    ATOM      46           6.7000000       3.3313060       0.0000000
    ATOM      47           9.0555890      -4.9969590       0.0000000
    ATOM      48           9.0555890      -2.4984800      -1.4424980
    ATOM      49           9.0555890      -2.4984800       1.4424980
    ATOM      50           9.0555890       0.0000000      -2.8849960
    ATOM      51           9.0555890       0.0000000       0.0000000
    ATOM      52           9.0555890       0.0000000       2.8849960
    ATOM      53           9.0555890       2.4984800      -1.4424980
    ATOM      54           9.0555890       2.4984800       1.4424980
END

BASIS
  type DZ
END

Relativistic Scalar ZORA

#Exchange-Correlation potential approximated by the Local Density Approximation.
XC
```

```
        LDA VWN
END

# Initialize Cartesian geometry optimization
GEOMETRY
    Optim Cartesian
    Branch new
END

eor

rm TAPE21 logfile
```

B Self-Energy Calculation Script

The following script is based on [20].

```
#!/bin/sh

# PART 1: Atomic Layer Construction

cp $ADFHOME/examples/adf/green_Al/Au.5p .
cp $ADFHOME/examples/adf/green_Al/Au.5p.dirac .

$ADFBIN/dirac < Au.5p.dirac
mv TAPE12 t12.rel

$ADFBIN/adf -n1 << eor
CREATE Au    file=Au.5p
RELATIVISTIC Scalar ZORA

COREPOTENTIALS t12.rel
End

XC
    LDA SCF VWN
END
eor
mv TAPE21 t21.Au

$ADFBIN/adf << eor
TITLE Gold atom
ATOMS
    Au          0.000000     0.000000     0.000000
END
RELATIVISTIC Scalar ZORA
FRAGMENTS
    Au  t21.Au
END
XC
    LDA SCF VWN
END
eor
mv TAPE21 Au.t21

# PART 2: Principal Layer Construction

$ADFBIN/adf << eor
TITLE Principal layer
ATOMS
    Au        -2.355588    -6.662612     0.000000
    Au        -2.355589    -4.164133    -1.442498
    Au        -2.355589    -4.164133     1.442498
    Au        -2.355589    -1.665653    -2.884996
    Au        -2.355589    -1.665653     0.000000
    Au        -2.355589    -1.665653     2.884996
    Au        -2.355589     0.832826    -1.442498
```

```
    Au       -2.355589    0.832826    1.442498
    Au       -2.355589    3.331306    0.000000
    Au        0.000000   -4.996959    0.000000
    Au        0.000000   -2.498480   -1.442498
    Au        0.000000   -2.498480    1.442498
    Au        0.000000    0.000000   -2.884996
    Au        0.000000    0.000000    0.000000
    Au        0.000000    0.000000    2.884996
    Au        0.000000    2.498480   -1.442498
    Au        0.000000    2.498480    1.442498
    Au        0.000000    4.996959    0.000000
    Au        2.355589   -3.331306    0.000000
    Au        2.355589   -0.832826   -1.442498
    Au        2.355589   -0.832826    1.442498
    Au        2.355589    1.665653   -2.884996
    Au        2.355589    1.665653    0.000000
    Au        2.355589    1.665653    2.884996
    Au        2.355589    4.164133   -1.442498
    Au        2.355589    4.164133    1.442498
    Au        2.355588    6.662612    0.000000
END
SYMMETRY NOSYM
RELATIVISTIC Scalar ZORA
FRAGMENTS
    Au  Au.t21
END
XC
    LDA SCF VWN
END
eor
mv TAPE21 layer.t21

# PART 3: Bulk Layer Construction

$ADFBIN/adf << eor
TITLE Bulk gold
ATOMS
    Au       -9.422355  -11.659571    0.000000 f=left
    Au       -9.422356   -9.161092   -1.442498 f=left
    Au       -9.422356   -9.161092    1.442498 f=left
    Au       -9.422356   -6.662612   -2.884996 f=left
    Au       -9.422356   -6.662612    0.000000 f=left
    Au       -9.422356   -6.662612    2.884996 f=left
    Au       -9.422356   -4.164133   -1.442498 f=left
    Au       -9.422356   -4.164133    1.442498 f=left
    Au       -9.422356   -1.665653    0.000000 f=left
    Au       -7.066767   -9.993918    0.000000 f=left
    Au       -7.066767   -7.495439   -1.442498 f=left
    Au       -7.066767   -7.495439    1.442498 f=left
    Au       -7.066767   -4.996959   -2.884996 f=left
    Au       -7.066767   -4.996959    0.000000 f=left
    Au       -7.066767   -4.996959    2.884996 f=left
    Au       -7.066767   -2.498479   -1.442498 f=left
    Au       -7.066767   -2.498479    1.442498 f=left
```

Au	−7.066767	0.000000	0.000000	f=left
Au	−4.711178	−8.328265	0.000000	f=left
Au	−4.711178	−5.829785	−1.442498	f=left
Au	−4.711178	−5.829785	1.442498	f=left
Au	−4.711178	−3.331306	−2.884996	f=left
Au	−4.711178	−3.331306	0.000000	f=left
Au	−4.711178	−3.331306	2.884996	f=left
Au	−4.711178	−0.832826	−1.442498	f=left
Au	−4.711178	−0.832826	1.442498	f=left
Au	−4.711179	1.665653	0.000000	f=left
Au	−2.355588	−6.662612	0.000000	f=center
Au	−2.355589	−4.164133	−1.442498	f=center
Au	−2.355589	−4.164133	1.442498	f=center
Au	−2.355589	−1.665653	−2.884996	f=center
Au	−2.355589	−1.665653	0.000000	f=center
Au	−2.355589	−1.665653	2.884996	f=center
Au	−2.355589	0.832826	−1.442498	f=center
Au	−2.355589	0.832826	1.442498	f=center
Au	−2.355589	3.331306	0.000000	f=center
Au	0.000000	−4.996959	0.000000	f=center
Au	0.000000	−2.498480	−1.442498	f=center
Au	0.000000	−2.498480	1.442498	f=center
Au	0.000000	0.000000	−2.884996	f=center
Au	0.000000	0.000000	0.000000	f=center
Au	0.000000	0.000000	2.884996	f=center
Au	0.000000	2.498480	−1.442498	f=center
Au	0.000000	2.498480	1.442498	f=center
Au	0.000000	4.996959	0.000000	f=center
Au	2.355589	−3.331306	0.000000	f=center
Au	2.355589	−0.832826	−1.442498	f=center
Au	2.355589	−0.832826	1.442498	f=center
Au	2.355589	1.665653	−2.884996	f=center
Au	2.355589	1.665653	0.000000	f=center
Au	2.355589	1.665653	2.884996	f=center
Au	2.355589	4.164133	−1.442498	f=center
Au	2.355589	4.164133	1.442498	f=center
Au	2.355588	6.662612	0.000000	f=center
Au	4.711179	−1.665653	0.000000	f=right
Au	4.711178	0.832826	−1.442498	f=right
Au	4.711178	0.832826	1.442498	f=right
Au	4.711178	3.331306	−2.884996	f=right
Au	4.711178	3.331306	0.000000	f=right
Au	4.711178	3.331306	2.884996	f=right
Au	4.711178	5.829785	−1.442498	f=right
Au	4.711178	5.829785	1.442498	f=right
Au	4.711178	8.328265	0.000000	f=right
Au	7.066767	0.000000	0.000000	f=right
Au	7.066767	2.498479	−1.442498	f=right
Au	7.066767	2.498479	1.442498	f=right
Au	7.066767	4.996959	−2.884996	f=right
Au	7.066767	4.996959	0.000000	f=right
Au	7.066767	4.996959	2.884996	f=right
Au	7.066767	7.495439	−1.442498	f=right
Au	7.066767	7.495439	1.442498	f=right

```
    Au        7.066767    9.993918    0.000000 f=right
    Au        9.422356    1.665653    0.000000 f=right
    Au        9.422356    4.164133   -1.442498 f=right
    Au        9.422356    4.164133    1.442498 f=right
    Au        9.422356    6.662612   -2.884996 f=right
    Au        9.422356    6.662612    0.000000 f=right
    Au        9.422356    6.662612    2.884996 f=right
    Au        9.422356    9.161092   -1.442498 f=right
    Au        9.422356    9.161092    1.442498 f=right
    Au        9.422355   11.659571    0.000000 f=right
END
SYMMETRY NOSYM
RELATIVISTIC Scalar ZORA
FRAGMENTS
    left    layer.t21
    center  layer.t21
    right   layer.t21
END
XC
    LDA SCF VWN
END
eor
mv TAPE21 bulk.t21

# PART 4: Self-Energy Calculation

$ADFBIN/green << eor
SURFACE bulk.t21
    FRAGMENTS center right
END
EPS -0.5 0 1000
ETA 1e-6
eor
mv SURFACE left.kf

$ADFBIN/green << eor
SURFACE bulk.t21
    FRAGMENTS center left
END
EPS -0.5 0 1000
ETA 1e-6
eor
mv SURFACE right.kf
```

C Transport Calculation Script

The following script is based on [19].

```
$ADFBIN/adf << eor

TITLE Helicene

#Coordinates of the molecule
ATOMS
        S       -4.7000000      0.0000000       0.00000000
        H       -3.9260727      1.21683611      1.61512875
        H       -3.39406067     -0.72582719     -2.64968388
        C       -3.29478703     0.20446611      -0.14789025
        C       -3.08367615     0.93548501      1.00062926
        C       -2.39536074     -0.64609709     -2.24560618
        C       -2.20059157     -0.15766099     -0.94449996
        C       -1.78604267     1.30361751      1.35656767
        H       -1.63929661     1.95619161      2.205756
        H       -1.50293858     -1.29106249     -4.039812
        C       -1.33731274     -1.01548009     -3.00769203
        C       -0.88460388     0.00915171      -0.44371432
        C       -0.70448321     0.85822241      0.6582093
        C       -0.03745295     -1.04477829     -2.47659288
        C       0.18254797      -0.69807759     -1.11826255
        H       0.28514938      1.16839221      0.96400214
        H       0.75639511      -1.82540739     1.40424856
        H       0.91849833      -1.52094629     -4.35156435
        C       1.07379568      -1.33648859     -3.2976265
        C       1.43006145      -1.15498419     -0.53783399
        C       1.60495816      -1.59813549     0.77354805
        C       2.32633965      -1.38639749     -2.79496668
        C       2.55422697      -1.25444789     -1.40860089
        C       2.86980455      -1.75249889     1.27011413
        H       3.00100497      -2.02587749     2.3081079
        H       3.16356536      -1.53259479     -3.46154986
        C       3.84179542      -1.31486749     -0.86926863
        C       3.98953912      -1.57283209     0.46556843
        S       4.7000000       0.0000000       0.00000000
        H       4.71061388      -1.16675399     -1.49402462
END
SYMMETRY NOSYM
RELATIVISTIC Scalar ZORA
BASIS
    type DZP
    core Large
    createOutput None
END
XC
    LDA SCF VWN
END

eor
mv TAPE21 molecule.t21
```

```
$ADFBIN/adf << eor

#The molecule sandwiched between the contacts. The left, molecule and right fragments
#are created.
TITLE Helicene_leads

ATOMS
     Au      -11.4111770     -6.6626120      0.00000000      f=left
     Au      -11.4111780     -4.1641330     -1.44249800      f=left
     Au      -11.4111780     -4.1641330      1.44249800      f=left
     Au      -11.4111780     -1.6656530     -2.88499600      f=left
     Au      -11.4111780     -1.6656530      0.00000000      f=left
     Au      -11.4111780     -1.6656530      2.88499600      f=left
     Au      -11.4111780      0.8328260     -1.44249800      f=left
     Au      -11.4111780      0.8328260      1.44249800      f=left
     Au      -11.4111780      3.3313060      0.00000000      f=left
     Au       -9.0555890     -4.9969590      0.00000000      f=left
     Au       -9.0555890     -2.4984800     -1.44249800      f=left
     Au       -9.0555890     -2.4984800      1.44249800      f=left
     Au       -9.0555890      0.0000000     -2.88499600      f=left
     Au       -9.0555890      0.0000000      0.00000000      f=left
     Au       -9.0555890      0.0000000      2.88499600      f=left
     Au       -9.0555890      2.4984800     -1.44249800      f=left
     Au       -9.0555890      2.4984800      1.44249800      f=left
     Au       -9.0555890      4.9969590      0.00000000      f=left
     Au       -6.7000000     -3.3313060      0.00000000      f=left
     Au       -6.7000000     -0.8328260     -1.44249800      f=left
     Au       -6.7000000     -0.8328260      1.44249800      f=left
     Au       -6.7000000      1.6656530     -2.88499600      f=left
     Au       -6.7000000      1.6656530      0.00000000      f=left
     Au       -6.7000000      1.6656530      2.88499600      f=left
     Au       -6.7000000      4.1641330     -1.44249800      f=left
     Au       -6.7000000      4.1641330      1.44249800      f=left
     Au       -6.7000010      6.6626120      0.00000000      f=left
     S        -4.7000000      0.0000000      0.00000000      f=molecule
     H        -3.9260727      1.21683611     1.61512875      f=molecule
     H        -3.39406067    -0.72582719    -2.64968388      f=molecule
     C        -3.29478703     0.20446611    -0.14789025      f=molecule
     C        -3.08367615     0.93548501     1.00062926      f=molecule
     C        -2.39536074    -0.64609709    -2.24560618      f=molecule
     C        -2.20059157    -0.15766099    -0.94449996      f=molecule
     C        -1.78604267     1.30361751     1.35656767      f=molecule
     H        -1.63929661     1.95619161     2.205756        f=molecule
     H        -1.50293858    -1.29106249    -4.039812        f=molecule
     C        -1.33731274    -1.01548009    -3.00769203      f=molecule
     C        -0.88460388     0.00915171    -0.44371432      f=molecule
     C        -0.70448321     0.85822241     0.6582093       f=molecule
     C        -0.03745295    -1.04477829    -2.47659288      f=molecule
     C         0.18254797    -0.69807759    -1.11826255      f=molecule
     H         0.28514938     1.16839221     0.96400214      f=molecule
     H         0.75639511    -1.82540739     1.40424856      f=molecule
     H         0.91849833    -1.52094629    -4.35156435      f=molecule
     C         1.07379568    -1.33648859    -3.2976265       f=molecule
     C         1.43006145    -1.15498419    -0.53783399      f=molecule
```

```
C       1.60495816    -1.59813549    0.77354805    f=molecule
C       2.32633965    -1.38639749    -2.79496668   f=molecule
C       2.55422697    -1.25444789    -1.40860089   f=molecule
C       2.86980455    -1.75249889    1.27011413    f=molecule
H       3.00100497    -2.02587749    2.3081079     f=molecule
H       3.16356536    -1.53259479    -3.46154986   f=molecule
C       3.84179542    -1.31486749    -0.86926863   f=molecule
C       3.98953912    -1.57283209    0.46556843    f=molecule
S       4.7000000     0.0000000      0.00000000    f=molecule
H       4.71061388    -1.16675399    -1.49402462   f=molecule
Au      6.7000000     -4.1641330     -1.44249800   f=right
Au      6.7000000     -4.1641330     1.44249800    f=right
Au      6.7000000     -1.6656530     -2.88499600   f=right
Au      6.7000000     -1.6656530     0.00000000    f=right
Au      6.7000000     -1.6656530     2.88499600    f=right
Au      6.7000000     0.8328260      -1.44249800   f=right
Au      6.7000000     0.8328260      1.44249800    f=right
Au      6.7000000     3.3313060      0.00000000    f=right
Au      6.7000010     -6.6626120     0.00000000    f=right
Au      9.0555890     4.9969590      0.00000000    f=right
Au      9.0555890     -4.9969590     0.00000000    f=right
Au      9.0555890     -2.4984800     -1.44249800   f=right
Au      9.0555890     -2.4984800     1.44249800    f=right
Au      9.0555890     0.0000000      -2.88499600   f=right
Au      9.0555890     0.0000000      0.00000000    f=right
Au      9.0555890     0.0000000      2.88499600    f=right
Au      9.0555890     2.4984800      -1.44249800   f=right
Au      9.0555890     2.4984800      1.44249800    f=right
Au      11.4111770    6.6626120      0.00000000    f=right
Au      11.4111780    4.1641330      1.44249800    f=right
Au      11.4111780    4.1641330      -1.44249800   f=right
Au      11.4111780    1.6656530      2.88499600    f=right
Au      11.4111780    -0.8328260     -1.44249800   f=right
Au      11.4111780    1.6656530      -2.88499600   f=right
Au      11.4111780    -0.8328260     1.44249800    f=right
Au      11.4111780    1.6656530      0.00000000    f=right
Au      11.4111780    -3.3313060     0.00000000    f=right

END
SYMMETRY NOSYM
RELATIVISTIC Scalar ZORA
FRAGMENTS
    left        layer.t21
    molecule    molecule.t21
    right       layer.t21
END
XC
    LDA SCF VWN
END

eor

mv TAPE21 fock.t21
```

```
#The calculation of the DOS and transmission.
$ADFBIN/green << eor
DOS fock.t21
TRANS fock.t21
EPS -0.5 0 1000
ETA 1e-6
LEFT left.kf
    FRAGMENT left
END
RIGHT right.kf
    FRAGMENT right
END
NOSAVE DOS_B, TRANS_B
eor
```

References

[1] Ron Naaman and David H. Waldeck. "Chiral-Induced Spin Selectivity Effect". In: *Journal of Physical Chemistry Letters* 3 (July 2012), pp. 2178–2187.

[2] Zouti Xie et al. "Spin Specific Electron Conduction through DNA Oligomers". In: *Nano Letters* 11 (2011), pp. 4652–4655.

[3] B. Göhler et al. "Spin Selectivity in Electron Transmission Through Self-Assembled Monolayers of Double-Stranded DNA". In: *Science* 331 (2011), pp. 894–897.

[4] J.M. Thijssen. *Lecture Notes Advanced Quantum Mechanics: A Quantum Mechanics Survival Guide*. TUDelft, 2013. Chap. 2.

[5] David J. Griffiths. *Introduction to Quantum Mechanics*. Cambridge University Press, 2017. ISBN: 9781107179868.

[6] David J. Griffiths. *Introduction to Electrodynamics*. Pearson Education Limited, 2014. ISBN: 9781292021423.

[7] J.M. Thijssen. *Computational Physics*. Cambridge University Press, 2007. Chap. 4.

[8] J.M. Thijssen. "Numerical Methods in Molecular Electronics". University Lecture. 2018.

[9] S. J. Clark. *Hartree-Fock Theory*. URL: http://cmt.dur.ac.uk/sjc/thesis_ppr/node8.html.

[10] L. J. Sham and W. Kohn. "One-Particle Properties of an Inhomogeneous Interacting Electron Gas". In: *Phys. Rev.* 145 (2 May 1966), pp. 561–567. DOI: 10.1103/PhysRev.145.561. URL: https://link.aps.org/doi/10.1103/PhysRev.145.561.

[11] J.M. Thijssen. *Computational Physics*. Cambridge University Press, 2007. Chap. 5.

[12] J.M. Thijssen. *Lecture Notes Advanced Quantum Mechanics: Green's functions in Quantum Mechanics*. TUDelft, 2013. Chap. 6.

[13] J.M. Thijssen. "Electron Transport Through Molecules". University Lecture. 2018.

[14] Chemistry LibreTexts. *Chirality and Stereoisomers*. Oct. 22, 2018. URL: https://chem.libretexts.org/Textbook_Maps/Organic_Chemistry/Supplemental_Modules_(Organic_Chemistry)/Chirality/Chirality_and_Stereoisomers.

[15] M. Hasan and V. Borovkov. *Conventional Aromatic Compounds and Helicene Compounds*. Feb. 12, 2018. URL: https://www.mdpi.com/2073-8994/10/1/10/htm#fig_body_display_symmetry-10-00010-f001.

[16] Unknown. *Optical Rotation*. Oct. 23, 2018. URL: https://en.wikipedia.org/wiki/Optical_rotation.

[17] M.P. Rebergen. "A Study of Induced Spin Selectivity in Chiral Molecules". MA thesis. TU Delft, 2018.

[18] G. te Velde et al. "Chemistry with ADF". In: *J. Comput. Chem.* 22.9 (2001), pp. 931–967. ISSN: 1096-987X. DOI: 10.1002/jcc.1056. URL: http://dx.doi.org/10.1002/jcc.1056.

[19] Unknown. *Example: Benzenedithiol junction*. Jan. 12, 2018. URL: https://www.scm.com/doc/ADF/Examples/green_BDT.html#example-green-bdt.

[20] Unknown. *Example: Gold electrodes*. Dec. 1, 2019. URL: https://www.scm.com/doc/ADF/Examples/green_Au.html#example-green-au.

[21] Unknown. *Fermi Energies, Fermi Temperatures, and Fermi Velocities*. URL: http://hyperphysics.phy-astr.gsu.edu/hbase/Tables/fermi.html.

[22] Unknown. *Run Types*. Feb. 2, 2019. URL: https://www.scm.com/doc/ADF/Input/Run_Types.html?highlight=runtype.

[23] Unknown. *GREEN: Non-self-consistent Green's function calculation*. URL: https://www.scm.com/doc/ADF/Input/GREEN.html.

[24] Yan-Zi Yu, Jian-Gang Guo, and Li-Jun Zhou. "Theoretical investigation on the adsorption and diffusion of lithium-ion on and between graphene layers with size and defect effects". In: *Adsorption Science Technology* 34.2-3 (2016), pp. 212–226. DOI: 10.1177/0263617415623429.

[25] MathWorks. *MatLab R2017b*. 2019. URL: https://www.mathworks.com/products/matlab.html.

[26] C. J. O. Verzijl, J. S. Seldenthuis, and J. M. Thijssen. "Applicability of the wide-band limit in DFT-based molecular transport calculations". In: *The Journal of Chemical Physics* 138.9 (2013), p. 094102. DOI: 10.1063/1.4793259.

[27] Steven H. Simon. *The Oxford Solid State Basics*. Oxford University Press, 2016. ISBN: 9780199680764.